Title: Heterogeneous timing of asexual cycles in *Plasmodium falciparum* quantified by extended time-lapse microscopy

Running title: Single-cell analysis of *Plasmodium* asexual cycles

Authors: Heungwon Park[1,2,3,+], Shuqiang Huang[3,4,5,+], Katelyn A. Walzer[3,6,+], Lingchong You[3,4], Jen-Tsan Ashley Chi[3,6,*], Nicolas E. Buchler[1,2,3,*,#]

Affiliations:

1. Department of Biology, Duke University, Durham, NC, USA 27708
2. Department of Physics, Duke University, Durham, NC, USA 27708
3. Center for Genomic & Computational Biology, Duke University, Durham, NC, USA 27710
4. Department of Biomedical Engineering, Duke University, Durham, NC, USA 27710
5. Shenzhen Institutes of Advanced Technology, Chinese Academy of Sciences. Shenzhen, China 518055
6. Department of Molecular Genetics & Microbiology, Duke University Medical Center, Durham, NC, USA 27710

+ These authors contributed equally to this work

*Senior co-authors: jentsan.chi@duke.edu, nicolas.buchler@duke.edu

#Corresponding author: nicolas.buchler@duke.edu

Abstract word count (<250 words): 224

Article word count (<5000 words, not including refs and fig legends): 3260

Abstract (< 250 words): (currently 224 words):

Malarial fever arises from the synchronous bursting of human red blood cells by the *Plasmodium* parasite. The released parasites re-infect neighboring red blood cells and undergo another asexual cycle of differentiation and proliferation for 48 hours, before again bursting synchronously. The synchrony of bursting is lost during *in vitro* culturing of the parasite outside the human body, presumably because the asexual cycle is no longer entrained by host-specific circadian cues. Therefore, most *in vitro* malaria studies have relied on the artificial synchronization of the parasite population. However, much remains unknown about the degree of timing heterogeneity of asexual cycles and how artificial synchronization may affect this timing. Here, we combined time-lapse fluorescence microscopy, long-term culturing and follow single cells to directly observe and measure the heterogeneous timing of *in vitro* asexual cycles. We first demonstrate that unsynchronized laboratory cultures are not fully asynchronous and the parasites exhibit a bimodal distribution in their first burst times. We then show that synchronized and unsynchronized cultures had similar asexual cycle periods, which indicates that artificial synchronization does not fundamentally perturb asexual cycle dynamics. Last, we demonstrate that sibling parasites descended from the same schizont exhibited significant variation in asexual cycle period, although smaller than the variation between non-siblings. The additional variance between non-siblings likely arises from the variable environments and/or developmental programs experienced in different host cells.

Importance (<150 words) (currently 149 words):

Human malaria affects hundreds of millions of people. One prominent feature of malaria is the periodic fever caused by circadian bursting of the parasites. Because circadian synchrony in parasite bursting is lost *in vitro*, most *Plasmodium* studies have relied on traditional bulk

population analysis using artificial synchronization. Much remains unknown about the heterogeneity of burst timing among parasites and the effects of synchronization. This gap in knowledge is partially due to the lack of longitudinal single-cell phenotyping. Here, we employed time-lapse fluorescence microscopy to monitor the parasite at single cell resolution. Our analysis of the temporal dynamics of its asexual cycle showed that the distribution of cycle times is similar between synchronized and unsynchronized populations, and that sibling parasites exhibit similar burst statistics to one another when compared to non-siblings. Collectively, these data illustrate the power of single cell analysis for addressing old and new questions in *P. falciparum*.

Introduction:

Malarial fever occurs in multiples of 24 hours. This circadian timing of fevers was already recognized by the ancients even when the cause of malaria remained mysterious. We now know that malarial fever arises from the synchronous bursting of host red blood cells by a eukaryotic parasite (*Plasmodium*). The released parasites called merozoites then infect neighboring red blood cells and undergo another asexual cycle where they use cellular resources to progress through an early ring-stage to trophozoite to schizont for a multiple-of-24 hours before again bursting synchronously. Circadian bursting of parasites from red blood cells is thought to be advantageous because it may help them overwhelm or avoid the host immune response (1, 2). Interestingly, *Plasmodium* species that cause malaria exhibit differences in the timing of their synchronous bursting. For example, the malarial fever that arises from *P. falciparum* has a 48-hour cycle, whereas *P. malariae* has a 72-hour cycle.

However, asexual cycles should lose synchrony with each other as intrinsic cell-to-cell variability in period leads to increasing differences in the timing and phase of events.

This was demonstrated by Trager and colleagues, who revolutionized malaria research by developing a protocol to culture and propagate *Plasmodium* outside of the body (3), and they showed that the synchrony of bursting was lost during *in vitro* culturing of parasites in flasks. Maintenance of synchronous bursting of *P. falciparum* during malaria infection likely arises from circadian host cues that periodically reset and entrain variable asexual cycles to a similar phase. This interpretation is supported by experiments that inverted the light-dark cycle experienced by hosts and showed that synchronous parasite bursting was subsequently inverted (4–6). Possible host cues that could affect the asexual cycle include temperature (7, 8), melatonin (9) and unknown factors.

Most research uses bulk assays to measure a biological signal averaged over many cells drawn from a population. The lack of synchrony in *in vitro* culturing poses a challenge for studying the asexual cycle because the signal of interest will be averaged over parasites in different stages. Thus, to study the asexual cycle in the laboratory using bulk assays, one must artificially synchronize the parasite population. One common method uses pulses of sorbitol to osmo-shock and kill parasites in the later stages of the asexual cycle and, thus, enrich for ring-stage parasites that span a window of time (10). This raises the following unanswered questions: What is the cell-to-cell variability in the asexual cycle period, and to what extent can it be minimized? Do artificially synchronized parasites exhibit similar cycle dynamics compared to unsynchronized parasites, or does sorbitol shock perturb the asexual cycle?

To unambiguously address these two questions, we employed time-lapse fluorescence microscopy and long-term culturing to image red blood cells infected with a GFP-transgenic parasite for longer than one asexual cycle. We used this single-cell assay to measure the

timing and variability in bursting of individual parasites either with or without sorbitol synchronization. By following the bursting of individual parasites and their descendants, we could also quantify whether siblings (merozoites that burst from the same founder schizont) had similar asexual cycle periods to non-siblings (merozoites that burst from different founder schizonts). Below, we present our experiments and data while leaving extensive interpretation for the Discussion.

Results:

Tracking parasite bursting using time-lapse microscopy. We modified a recent time-lapse microscopy protocol (11) to measure the parasite bursting over 80 hours and determine cell-to-cell variability of the asexual cycle in *P. falciparum*. We customized wells in a Corning culture bottle; see Materials & Methods. Briefly, glass slides in the wells were coated with Concanavalin A (0.5 mg/ml), washed with PBS and loaded with 300 µl of red blood cells (RBC) that were infected by synchronized or unsynchronized GFP-transgenic parasites. The synchronized parasites were prepared using two rounds of sorbitol shock (10). After loading the infected red blood cells, we washed out non-adherent cells, filled the bottle with nutrient medium and blood gas, and left it closed and unperturbed for the remainder of the experiment. We used fluorescence microscopy in a temperature control microscope (37 °C) to monitor the timing of burst and re-invasion events, e.g. parasite right before (Fig 1A) and after (Fig 1B) bursting the host RBC. Because the merozoites released from a burst would locally re-infect RBCs, we could follow a full asexual cycle from the first burst of the schizont "founder" cell (burst time t_i of the ith founder) to the subsequent bursts of those RBCs infected by progeny GFP-merozoites (burst time $t_{i,k}$ of the kth progeny descended from the ith founder) (Fig 1C, D, E, and F). Such data permit the quantification of variability in the timing of bursts over one asexual cycle; see labeling scheme in Fig 1G.

Variability of parasite burst times in synchronized and unsynchronized cells. We started by analyzing the elapsed time between the start of the experiment until the first recorded RBC burst of the founder parasites (t_i) in synchronized and unsynchronized populations (Fig 2). All experiments were done twice and the first-burst statistics were identical between replicates (Fig S1). In the synchronized culture, ~80% of total parasites undergo bursting within the first 10 hours (mean is 6.8 hours and standard deviation is 4.1 hours) displayed either as frequency (Fig 2A) or individual dots (Fig 2B). Surprisingly, the first-burst times of the unsynchronized population were not entirely random or asynchronous (i.e. equally likely to burst at any given time). Rather, the unsynchronized population exhibited two well-defined modes at ~11 hours and ~39 hours. The biological replicate also had a bimodal distribution with similar timing (Fig S1).

Measuring asexual cycles at the single cell level. Next, we measured asexual cycle periods of parasites with or without synchronization (Fig 3A, C, respectively) by quantifying the difference in the first-burst time of the founder cell (t_i, i^{th} founder) and the second-burst time of its progeny ($t_{i,k}$, k^{th} descendant of ith founder). The asexual cycle periods in the synchronized and unsynchronized parasites were statistically indistinguishable and had a mean of ~55 hours (Fig 3B, D, respectively). The asexual cycle periods of the synchronized and unsynchronized parasites in the biological replicate were similar with a mean of ~58 hours (Fig. S2), which is slightly longer than the first replicate. However, both periods were consistently longer than the synchronous 48-hour asexual cycle of *P. falciparum* that occurs during malarial fever in human hosts, a point that we revisit in our discussion.

Comparison of asexual cycles between siblings and non-siblings. With our unique ability to trace the lineage of the parents and progeny, we sought to compare the asexual cycle periods of siblings (merozoites from the same founder schizont) and non-siblings (merozoites from different founder schizonts). We plotted the asexual cycle time of siblings (grouped by founder) for the synchronized population; see Fig. 4. We found that there were two layers of variation. Siblings, which initially burst from the same founder cell and start tightly synchronized, still exhibit variation in the timing of downstream events and their asexual cycle period. These differences are termed "sibling variance". In addition, the progeny of different founders exhibit additional variation in their asexual cycle time, which we termed "founder variance". To estimate these two variances, we considered a simple model $\tau_{i,k} = \tau_i + \tau_k$ where the first term (asexual cycle time of founder) and second term (sibling variance about the founder asexual cycle time) are drawn from a normal distribution $N(\tau, {\sigma_i}^2)$ and $N(0, {\sigma_k}^2)$, respectively. We first verified that τ_i and τ_k were normally distributed using a Shapiro-Wilks test (p-value > 0.2 for all data sets) and then estimated τ, σ_i, σ_k; see Table 1. The variability in asexual cycle between siblings (σ_k) was less than or equal to the additional variability that arises from founders (σ_i) across all conditions and replicates. These data demonstrate that the variability in the asexual cycle period between siblings (σ_k) ranges from 2-4 hours and that non-siblings (i.e. most of the population) have an additional source of variability (σ_i) due to founder effects.

Discussion:

We used timelapse fluorescence microscopy of GFP-expressing *P. falciparum* to quantify the timing and variability of the asexual cycle in *in vitro* culturing conditions. For the first time, we measured the first-burst time of individual founder parasites, local reinfection, and second-burst times of progeny (Fig. 1) for unsynchronized and sorbitol-

synchronized parasites. As expected, the synchronized population exhibited a unimodal distribution of first-burst times with variance due to imperfect synchronization and/or dephasing since the last sorbitol synchronization (Fig. 2A). Surprisingly, the unsynchronized population exhibited a bimodal distribution of first-burst times with two peaks separated by ~28 hours (Fig. 2B and S1). The measured asexual cycle period was unimodal with a mean between 54-58 hours (Fig. 3 and S2), which is longer than the 28-hour difference in the two peaks in the unsynchronized population. The implications are two-fold: (i) *in vitro* cultures may not be perfectly asynchronous, as often assumed, and (ii) our routine culturing appears to create two staggered cohorts of founder parasites in the unsynchronized population. The reason for our bimodal distribution is unknown. One explanation may be that laboratory parasites are cultured by human researchers whose activities are circadian-regulated and our routine lab manipulations synchronize and split the ~56-hour asexual cycle population into two cohorts separated by ~24 hours. Another possibility is that the parasites self-organize into two separate cohorts via cell-to-cell communication, e.g. exosomes secreted from the infected RBC (12), such that the split population exhibits a 1:2 relationship with the intrinsic asexual cycle period (28 hour gap between cohorts versus ~56 hours asexual cycle). Future experiments could distinguish between these possibilities by culturing parasites in human-free, continuous culture (e.g. bioreactors) and/or changing the mean asexual cycle period by using different strains; see below.

We then quantified the cell-to-cell variability in the asexual cycle period by measuring the time interval between the first burst of each founder and second bursts of its progeny. These single-cell cells experiments are novel because, for the first time, we measured asexual cycles for parasites in an unsynchronized population. Our results reassuringly show that sorbitol synchronization does not fundamentally perturb the asexual

cycle because the mean cycle periods were similar in synchronized and unsynchronized conditions (Fig. 3). The mean period of the GFP-labelled parasites was ~15% longer than 48 hours, a difference that might arise from the burden of GFP expression, RBC immobilization, and/or the photo-toxicity from extended timelapse fluorescence imaging. However, our results are consistent with previous *in vitro* studies showing that different *P. falciparum* strains have mean asexual cycle periods that are both shorter (13–16) or longer (13) than the synchronous 48-hour cycle that occurs during malaria in the human host. Such differences have interesting mechanistic implications because shorter or longer period strains would have to be delayed or advanced, respectively, by the host circadian cues to entrain to a 48-hour period. In the future, it would be interesting to understand how other *Plasmodium* strains and species with intrinsically shorter and longer *in vitro* asexual cycle periods proliferate and synchronize in non-human hosts (e.g. mouse) dominated by a circadian rhythm.

Last, our single-cell assays permitted us to compare sibling and non-sibling asexual cycle times and directly quantify sources of cell-to-cell variability. We made several observations. First, the variability in the asexual cycle period between siblings (σ_k) ranged from 2-4 hours (Table 1). This is a fundamental measurement because it shows that siblings, which are as uniformly staged as parasites can possibly get (i.e. same host cell, developmental sequence), accumulate 2-4 hour differences in their asexual cycle times within one generation. Second, non-siblings had more cell-to-cell variability in their asexual cycle than siblings because of an additional source of variation specific to each founder (σ_i); see Fig. 4 and Table 1. This variation, which further increases the cell-to-cell variation present in a population of parasites, likely arises from heterogeneities between founders, e.g. age, molecular factors, epigenetic states, or host cell environment. Third, although the mean asexual cycle time was unaffected by culturing conditions, artificial synchronization reduced

both sibling and founder variation in the asexual cycle period by two-fold (Table 1). The mechanism for this variance reduction is unknown, but selection for ring-stage parasites could reduce asexual cycle variability by affecting cell physiology and/or the population demographics sensed through cell-cell communication.

We envision extended time-lapse imaging could be applied to answer other questions. For example, one could capture and monitor infrequent, but important, cell-fate events, such as the small proportion (<5%) of parasites that commit to a sexual fate and develop into male or female gametocytes. It would also be possible to use multiple fluorescent and luminescent reporter genes under the control of genes involved in gametocyte commitment to monitor the regulated expression of these genes over extended periods of time or various environmental cues. Extended time-lapse imaging could also be used to measure the wide variety of gene expression and genetic noise inherent in *P. falciparum* and other parasites, as well as the heterogeneous responses of single parasites to drug treatment and environmental stress.

Materials & Methods:

Parasite strain and laboratory culturing. Strain 3D7HT-GFP, which constitutively expresses GFP (17), was obtained from the Malaria Research and Reference Reagent Resource Center (MR4). The reagent was verified by the original contributors before submission to MR4 and we subsequently confirmed phenotype (i.e. GFP expression) with flow cytometry and fluorescence microscopy. Parasites were thawed from frozen stock and cultured in human B+ erythrocytes at 4% hematocrit according to standard procedures (3) using RPMI 1640 medium with 0.5% AlbuMAX II. Blood was drawn from donors under the institution approved IRB protocols. Old medium was changed and replaced every 24 hours

with fresh RPMI medium, and fresh erythrocytes were usually added every other cycle (48 hours) to keep the parasitemia below 5%. Medium change and/or erythrocyte addition were done in the middle of the day (10 AM - 2 PM) over a period of 1-2 hours in a cell culture hood at room temperature. The cell culture flask was filled with blood gas mixture (5% carbon dioxide, 5% oxygen, balance nitrogen), sealed, and returned to the incubator at 37°C.

Synchronization of the parasites. To obtain synchronous cultures, parasites were treated with 5% D-sorbitol which selects for parasites in the late ring stage (10). Sorbitol treatment was repeated twice, approximately 48 hours apart, to obtain synchronous cultures. After the last D-sorbitol treatment, synchronized cultures were grown to the trophozoite stage and placed at 5 – 10% parasitemia for imaging as previously described (11). In brief, 500 µL of parasite culture was centrifuged in a 15-mL Falcon tube at 1000 x g for 30 s on low brake. The supernatant was removed, and the pellet was washed twice in 1 mL of 1x PBS with centrifugations at 1000 x g for 30 s. The pellet was resuspended in 500 µL of RPMI 1640 medium supplemented with 25 mM HEPES, 12 mM NaHCO3, 6 mM D-glucose, 0.5% AlbuMAX II, and 0.2 mM hypoxanthine, and transferred to a 1.5-mL eppendorf tube (18). In parallel, we prepared unsynchronized cultures from the same initial parasite population.

Fabrication of the culturing device. We customized a 25 cm^2 Corning culture bottle for long-term imaging and culturing of samples. We first cut two 10 mm x 10 mm square holes on the bottom of the culture bottle with a spacing of 5 mm. We then sealed a No. 1 glass cover of 25 mm x 40 mm (VWR) to the bottom using aquarium silicone sealant (MARINELAND) (11) to form two independent wells. After solidifying the sealant overnight, we added 15 mL 70% ethanol for 1 hour to sterilize the surface of wells and interior of the

culturing bottle. The ethanol was subsequently removed by vacuuming the device (RobinAir VacuMaster) in a desiccator for 1 hour.

Time-lapse microscopy. We washed the wells twice using 300 µL 1X PBS (Gibco: DPBS(1x), Dulbecco's Phosphatase Buffered Saline, [+] Calcium Chloride and [+] Magnesium Chloride). To immobilize the red cells (11) to the glass surface, we coated the well with 0.5 mg/ml Concanavalin A from Canavalia ensiformis (Jack bean) Type IV-S (lyophilized powder, aseptically processed, Sigma-Aldrich). Each well was loaded with 300 µL of Concanavalin A solution (dissolved in water) and incubated for 10-20 min at 37°C with the bottle cap fully closed. Concanavalin A was subsequently pipetted out and the wells were washed with 1X PBS twice. We immediately loaded 300 µL of culture synchronized or unsynchronized parasites into each well and incubated for 10 min at 37°C to allow the cells to settle on the surface. Non-immobilized cells were removed and immobilized cells were then further washed by 1X PBS to achieve a monolayer of red cells under the microscope. We added 20 mL of supplemented RPMI 1640 medium. This phenol red-free RPMI medium reduces photo-toxicity (18). Mixed blood gas was purged into the culture bottle for 1 min at a pressure of about 3 psi before capping and sealing the culture bottle.

We used a temperature-controlled, DeltaVision Elite microscope with a 60x/1.25 numerical aperture phase-contrast oil objective. Images were acquired with an Evolve EMCCD camera (Photometrics, Tucson, AZ) with 10 MHz speed, 1x1 binning, 10x gain, and 512x512 dpi. Our culturing device was fixed to the microscope stage and the incubation chamber was maintained at 37°C during the entire experiment. To minimize light exposure on the samples, we used 32% transmission efficiency with 0.01-second exposure time for transmitted light, and 2% transmission with 0.025-second exposure for FITC (GFP). Filter set 2 (Polychroic

BGmCherry, FR (alexaquad) DAPI, FITC, AF594, CY5) and Alexa mode were chosen to further refine the FITC signal from the microscope settings. Images were collected every 6 minutes for 80 - 120 hours at 40-50 different positions across the two wells. We used the DeltaVision UltimateFocus™ module to compensate for thermal drift and maintain cells in the z-focal plane.

Image analysis. Phase and GFP images were merged using Image J (19) to visualize the asexual cycle dynamics of GFP-tagged malaria parasites bursting, reinfecting, proliferating, and re-bursting red blood cells. We subtracted each background from Phase images and GFP images by using the "Subtract Background" function in the Image J and then merged both images in all time-frames. Once we had the time-sequences of the merged images, we checked frame-by-frame to determine the frame in which the parasite burst occurred. During the whole image tracking procedure, we did not change the contrast, but for some frames when parasite bursting was not clear due to low GFP signal, we adjusted the contrast until we got visually clear parasite images and bursting. Our image analysis of asexual cycle dynamics was limited to 80+ hours because uninfected red blood cells started lysing. The spontaneous lysis of red blood cells makes it difficult to distinguish between bursting and lysing in these late time points. We only considered schizont rupture and merozoite release as parasite bursting. Bursting that occurred at earlier stages, such as during the ring or trophozoite stage, was considered hemolysis of the red blood cell.

Acknowledgements: This work was funded by a seed grant from the Duke Center for Genomic & Computational Biology (NEB and JTC), Duke MGM Chair Pilot Fund, Duke Chancellor Award, a National Science Foundation Graduate Research Fellowship (KAW), a National Institutes of Health Director's New Innovator Award DP2 OD008654-01 (NEB),

and a Burroughs Wellcome Fund Pathogenesis (JTC) and CASI Award BWF 1005769.01 (NEB).

Author contributions: HP, SH, KAW, JTC, NEB conceived of the project; KAW cultured and synchronized strains; HP, SH fabricated culturing device; HP, SH performed timelapse fluorescence microscopy; HP, NEB analyzed the data; HP, KAW, JTC, NEB drafted initial manuscript; all authors revised and approved of the final manuscript.

References:

1. **O'Donnell AJ**, **Schneider P**, **McWatters HG**, **Reece SE**. 2011. Fitness costs of disrupting circadian rhythms in malaria parasites. Proc Biol Sci **278**:2429–2436.

2. **Mideo N**, **Reece SE**, **Smith AL**, **Metcalf CJE**. 2013. The Cinderella syndrome: why do malaria-infected cells burst at midnight? Trends Parasitol **29**:10–16.

3. **Trager W**, **Jensen JB**. 1976. Human malaria parasites in continuous culture. Science **193**:673–675.

4. **Taliaferro WH**, **Taliaferro LG**. 1934. Alteration in the time of sporulation of Plasmodium brasilianum in monkeys by reversal of light and dark. Am J Hyg **20**:50–59.

5. **Stauber LA**. 1939. Factors influencing the asexual periodicity of avian malarias. J Parasitol **25**:95.

6. **Young MD**, **Coatney GR**, **Stubbs TH**. 1940. Studies on induced quartan malaria in negro paretics: II. The effect of modifying the external conditions. Am J Hyg **32**:63.

7. **Hawking F**, **Worms MJ**, **Gammage K**. 1968. Host temperature and control of 24-hour and 48-hour cycles in malaria parasites. The Lancet.

8. **Kwiatkowski D**. 1989. Febrile temperatures can synchronize the growth of Plasmodium falciparum in vitro. J Exp Med **169**:357–361.

9. **Hotta CT**, **Gazarini ML**, **Beraldo FH**, **Varotti FP**, **Lopes C**, **Markus RP**, **Pozzan T**, **Garcia CR**. 2000. Calcium-dependent modulation by melatonin of the circadian rhythm in malarial parasites. Nat Cell Biol **2**:466–468.

10. **Lambros C**, **Vanderberg JP**. 1979. Synchronization of Plasmodium falciparum erythrocytic stages in culture. J Parasitol **65**:418–420.

11. **Grüring C**, **Heiber A**, **Kruse F**, **Ungefehr J**, **Gilberger T-W**, **Spielmann T**. 2011. Development and host cell modifications of Plasmodium falciparum blood stages in four dimensions. Nat Commun **2**:165.

12. **Regev-Rudzki N**, **Wilson DW**, **Carvalho TG**, **Sisquella X**, **Coleman BM**, **Rug M**, **Bursac D**, **Angrisano F**, **Gee M**, **Hill AF**, **Baum J**, **Cowman AF**. 2013. Cell-cell communication between malaria-infected red blood cells via exosome-like vesicles. Cell **153**:1120–1133.

13. **Reilly HB**, **Wang H**, **Steuter JA**, **Marx AM**, **Ferdig MT**. 2007. Quantitative dissection of clone-specific growth rates in cultured malaria parasites. Int J Parasitol **37**:1599–1607.

14. **Rovira-Graells N**, **Aguilera-Simón S**, **Tintó-Font E**, **Cortés A**. 2016. New Assays to Characterise Growth-Related Phenotypes of Plasmodium falciparum Reveal Variation in Density-Dependent Growth Inhibition between Parasite Lines. PLoS ONE **11**:e0165358.

15. **Liu J**, **Gluzman IY**, **Drew ME**, **Goldberg DE**. 2005. The role of Plasmodium falciparum food vacuole plasmepsins. J Biol Chem **280**:1432–1437.

16. **Mancio-Silva L**, **Lopez-Rubio JJ**, **Claes A**, **Scherf A**. 2013. Sir2a regulates rDNA transcription and multiplication rate in the human malaria parasite Plasmodium falciparum. Nat Commun **4**:1530.

17. **Talman AM**, **Blagborough AM**, **Sinden RE**. 2010. A Plasmodium falciparum strain expressing GFP throughout the parasite's life-cycle. PLoS ONE **5**:e9156.

18. **Grüring C**, **Spielmann T**. 2012. Imaging of live malaria blood stage parasites. Meth Enzymol **506**:81–92.

19. **Schneider CA**, **Rasband WS**, **Eliceiri KW**. 2012. NIH Image to ImageJ: 25 years of image analysis. Nat Methods **9**:671–675.

Figure Legends: ("Legends should provide enough information so that the figure is understandable without frequent reference to the text")

Figure 1: Time-lapse fluorescence microscopy of parasite asexual cycles. (A-F) We measured the asexual cycles of GFP-labeled parasites with phase contrast and GFP fluorescence images taken every 6 minutes (0.1 h). We followed bursting, local reinfection of new red blood cells, asexual growth and division, and re-bursting. (A) Example of an infected

red blood cell (e.g. founder cell i) that is about to burst (yellow arrow). (B) Parasite bursting from founder cell i (time of first-burst, t_i). (C) Progeny parasites re-infect neighboring red blood cells, proliferate asexually, and the first of the progeny (yellow arrow) is about to burst. (D) Parasite bursting from progeny 1 of founder cell i (time of second-burst, $t_{i,1}$). (E) The second of the progeny (yellow arrow) is about to burst. (F) Parasite bursting from progeny 2 of founder cell i (time of second-burst, $t_{i,2}$). (G) Notation for parasite bursting. Founder cell i bursts at time t_i, some progeny re-infect red blood cells, undergo an asexual cycle, and burst at time $t_{i,1}$ (first progeny to burst), $t_{i,2}$ (second progeny to burst), $t_{i,3}$ (third progeny to burst), etc. The asexual cycle period ($\tau_{i,k}$) of progeny k of founder cell i is ($t_{i,k}$ - t_i), i.e. burst-to-burst time interval.

Figure 2: First-burst times of founder cells in synchronized and unsynchronized populations. We plot the first-burst times (t_i) of initially-infected founder cells in sorbitol-synchronized (A and B, n=60 founder cells) and unsynchronized (C and D, n=79 founder cells) cultures. B and D plot first-burst times (t_i, x-axis) ordered by founder cell (i, y-axis). For circadian reference, perpendicular dotted lines indicate a real world time (i.e. midnight). A and C show the normalized distributions of the burst times in B and D (bin size = 5 hours). Biological replicate is shown in Fig. S1 and complete data are available in Dataset S1. This figure includes founder cells that burst, but whose progeny could not be confidently identified or were unable to re-infect red blood cells (i.e. no $t_{i,k}$ and, thus, no measured asexual cycle).

Figure 3: Asexual cycle period in synchronized and unsynchronized cells. We plotted the founder first-burst times (t_i), progeny second-burst times ($t_{i,k}$), and asexual cycle period ($t_{i,k}$-t_i) for sorbitol-synchronized (A and B, n=61 founder-progeny pairs) and unsynchronized (C and

D, n=22 founder-progeny pairs) cultures. A and C show the first-burst times of the founder cells (t_i, dots on y-axis) and second-burst times of the progeny ($t_{i,k}$, triangles on y-axis) of each founder cell (i, x-axis). Progeny cells from the same founder cell (i.e. siblings) are linked and colored contiguously in alternating patterns of red and blue. B and D show the normalized distributions of asexual cycle period (burst-to-burst interval, $\tau_{i,k} = t_{i,k} - t_i$) measured from A and C. The numbers show the mean and standard deviation of asexual cycle period. Bin size is 5 hours. Two-sample Kolmogorov-Smirnov test and Wilcoxon rank sum test indicate that asexual cycle period distributions are similar between the synchronized and unsynchronized population (p-value $_{KS}$ = 0.39, p-value $_{W}$ = 0.31). A biological replicate is shown in Fig. S2, and asexual cycle data are available in Dataset S1.

Figure 4: Variance in asexual cycle period between siblings and non-siblings. A plot of asexual cycle period $\tau_{i,k}$ within each sibling group (doublet, triplet, and quadruplet) from the synchronized population. The mean period of each sibling group (τ_i) is shown with circle-plus symbol and projected to the right to display the full distribution of founder times. We estimated the variance in asexual cycle between siblings (σ_k) by averaging over all sibling groups. The distribution of τ_i (right) was used to estimate average period (τ) and the variance in asexual cycle between founders (σ_i).

Table 1: Estimate of founder-specific and sibling-specific variance in asexual cycle period across conditions and replicates. We could not estimate sibling-specific variance in unsynchronized Replicate 2 because it did not have sibling groups (i.e. no doublet or higher).

	Synchronized Replicate 1	Unsynchronized Replicate 1	Synchronized Replicate 2
τ	54.0 h	57.5 h	57.3 h

σ_i	2.9 h	4.9 h	2.7 h
σ_k	1.7 h	5.0 h	2.7 h

Supplementary materials

Movie S1. Timelapse fluorescence movie of GFP-labelled parasites.

Dataset S1: First-burst time, second-burst time, and asexual cycle period of synchronized and unsynchronized parasites for both biological replicates.

Figure S1. First burst time of founder cells in synchronized and unsynchronized populations are similar between replicates.

We plot the first-burst times (t_i) of initially-infected founder cells in sorbitol-synchronized (A and B, n=64 founder cells) and unsynchronized (C and D, n=62 founder cells) cultures of a biological replicate. B and D plot first-burst times (t_i, x-axis) of founder cells (i, y-axis). For circadian reference, perpendicular dotted lines indicate a real-world time (i.e. midnight). A and C show the normalized distributions of the burst times in B and D (bin size = 5 hours). Biological replicate is shown in Fig. 2, and complete data are available in Dataset S1. Two-sample Kolmogorov-Smirnov test and Wilcoxon rank sum test indicate that synchronized (p-value $_{KS}$ = 0.96, p-value $_W$ = 0.48) and unsynchronized (p-value $_{KS}$ = 0.42, p-value $_W$ = 0.22) first-burst time distributions are similar between replicates.

Figure S2. Asexual cycle period in synchronized and unsynchronized populations are similar within a replicate, but differ between replicates. We plotted the founder first-burst times (t_i), progeny second-burst times ($t_{i,k}$), and asexual cycle period ($t_{i,k}$-t_i) for sorbitol-

synchronized (A and B, n=25 founder-progeny pairs) and unsynchronized (C and D, n=9 founder-progeny pairs) cultures. A and C show the first-burst times of the founder cells (t_i, dots on y-axis) and second-burst times of the progeny ($t_{i,k}$, triangles on y-xis) of each founder cell (i, x-axis). Progeny from the same founder cell (i.e. siblings) are linked and colored contiguously in alternating patterns of red and blue. B and D show the normalized distributions of asexual cycle period (burst-to-burst interval, $\tau_{i,k} = t_{i,k} - t_i$) measured from A and C. The numbers show the mean and standard deviation of asexual cycle period. Bin size is 5 hours. Two-sample Kolmogorov-Smirnov test and Wilcoxon rank sum test indicate that asexual cycle period distributions of the synchronized and unsynchronized population are similar (p-value $_{KS}$ = 0.86, p-value $_W$ = 0.81). However, the distribution of the synchronized population is significantly different between biological replicates (p-value $_{KS}$ = 8.6×10^{-5}, p-value $_W$ = 6.3×10^{-5}). Biological replicate is shown in Fig. 3, and asexual cycle data are available in Dataset S1.

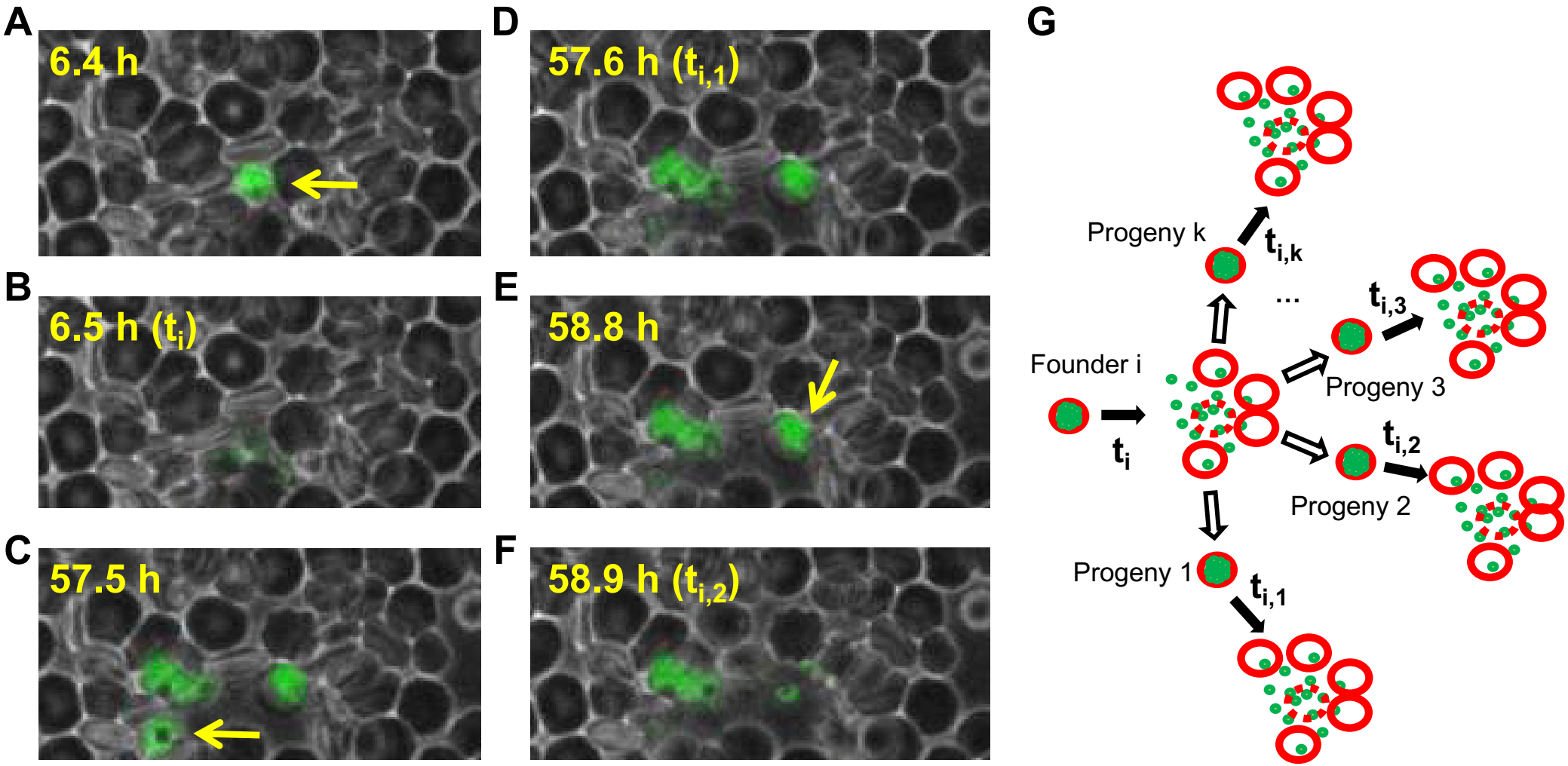
A
6.4 h
B
6.5 h (t_i)
C
57.5 h
D
57.6 h ($t_{i,1}$)
E
58.8 h
F
58.9 h ($t_{i,2}$)
G
Founder i
t_i
Progeny 1
$t_{i,1}$
Progeny 2
$t_{i,2}$
Progeny 3
$t_{i,3}$
...
Progeny k
$t_{i,k}$

Figure 1

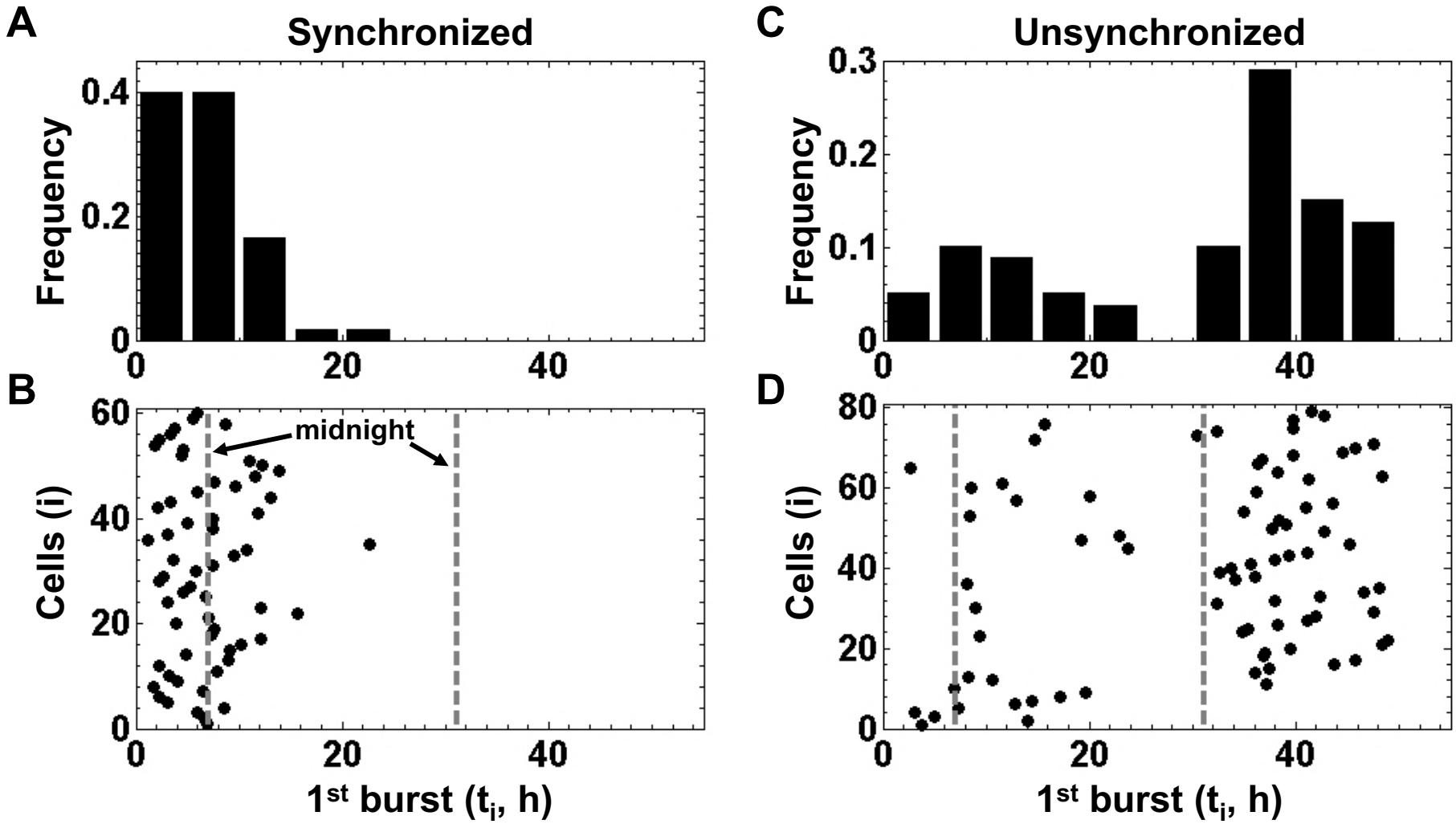
A
Synchronized
Frequency
0.4
0.2
0
0
20
40
B
Cells (i)
60
40
20
0
midnight
1st burst (ti, h)
C
Unsynchronized
Frequency
0.3
0.2
0.1
D
Cells (i)
80
60
40
20

Figure 2

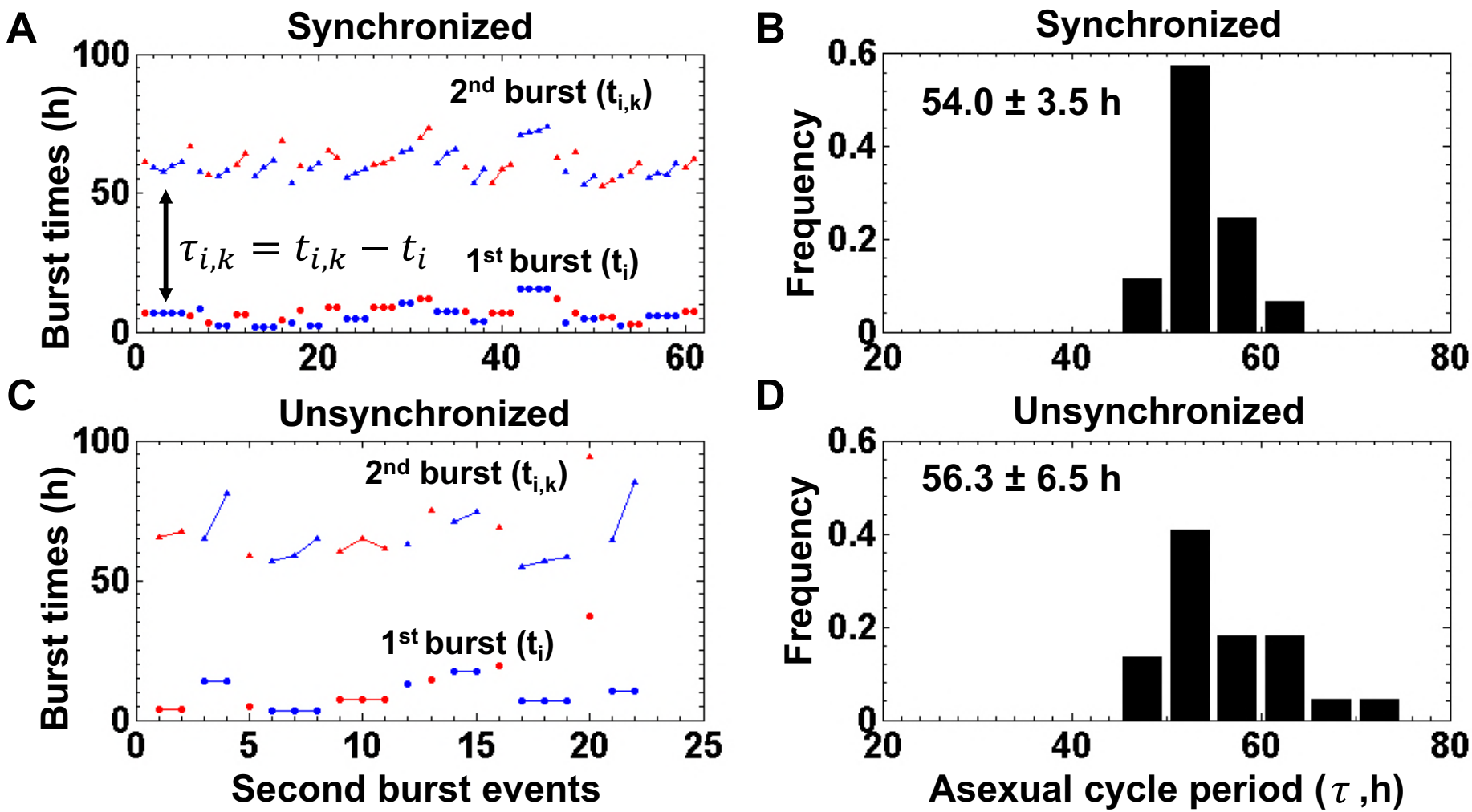
A
Synchronized
Burst times (h)
2nd burst (ti,k)
1st burst (ti)
$\tau_{i,k} = t_{i,k} - t_i$
B
Synchronized
Frequency
54.0 ± 3.5 h
C
Unsynchronized
Burst times (h)
2nd burst (ti,k)
1st burst (ti)
Second burst events
D
Unsynchronized
Frequency
56.3 ± 6.5 h
Asexual cycle period (τ ,h)

Figure 3

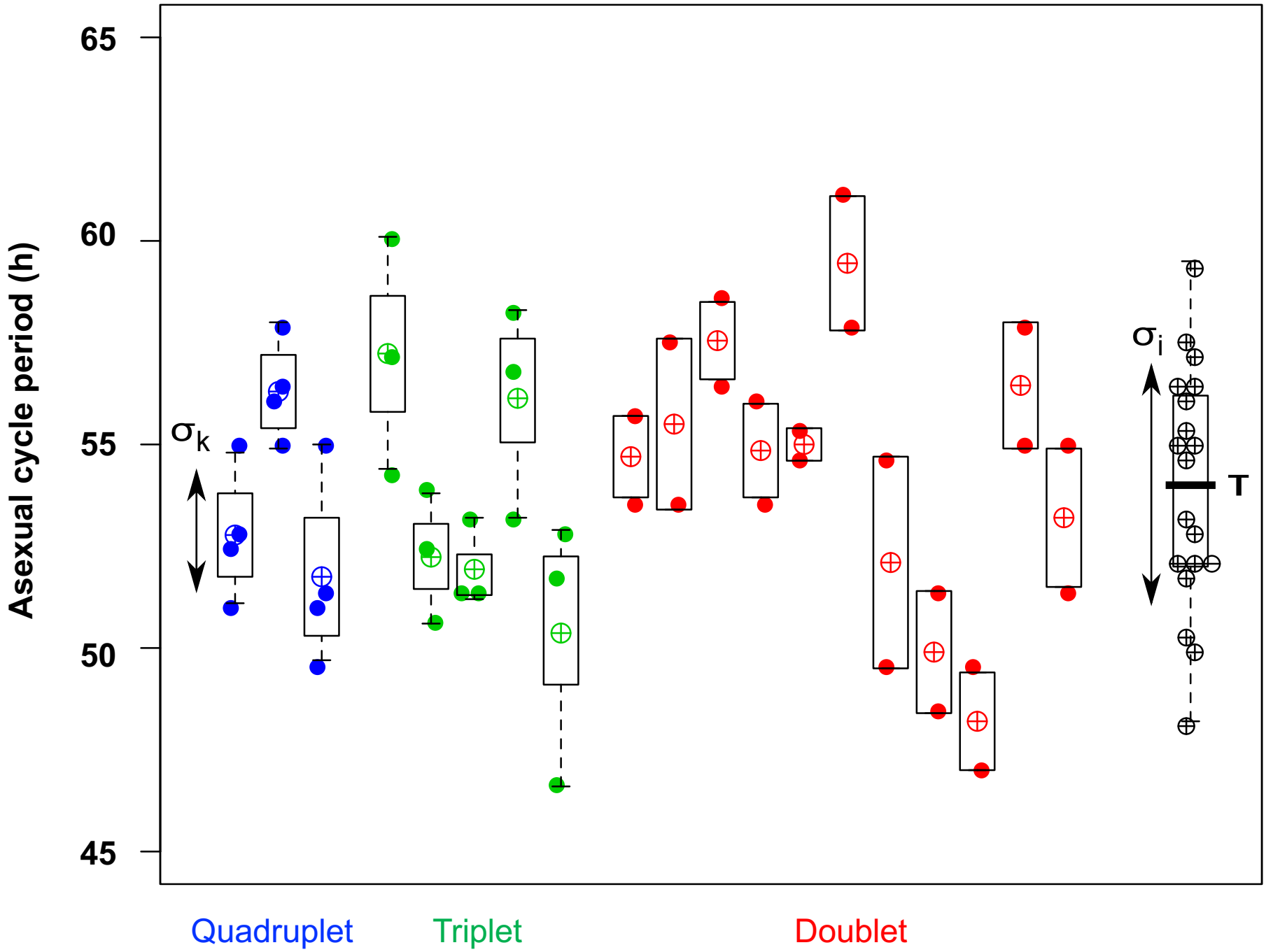
Asexual cycle period (h)
65
60
55
50
45
σk
σi
T
Quadruplet
Triplet
Doublet

Figure 4